Suárez, M.; Fernández-González, D.; Gutiérrez-González, C.; Díaz, L.; Borrell Tomás, MA.; Moya, J.; Torrecillas, R.... (2022). Effect of green body density on the properties of graphite-molybdenum-titanium composite sintered by spark plasma sintering. Journal of the European Ceramic Society. 42(5):2048-2054. https://doi.org/10.1016/j.jeurceramsoc.2021.12.073

Effect of Green Body Density on the Properties of Graphite-Molybdenum-Titanium Composite Sintered by Spark Plasma Sintering

Authors: M. Suárez [a,*], D. Fernández-González [a,†], C. F. Gutiérrez-González [b], L. A. Díaz [a], A. Borrell [c], J. S. Moya [a], A. Fernández [a]

Affiliations:

[a] Nanomaterials and Nanotechnology Research Center (CINN-CSIC), Universidad de Oviedo (UO), Principado de Asturias (PA), Avda. de la Vega, 4-6, 33940, El Entrego, Spain.

[b] Nanoker Research S.L. Polígono Industrial de Olloniego, parcela 22ª, Nave 5, Oviedo, 33660 Asturias, Spain.

[c] Instituto de Tecnología de Materiales, Universitat Politècnica de València (UPV), Camino de Vera S/N, 46022, Valencia, Spain.

Abstract:

This manuscript contains an experimental study about the effect of the degree of compaction of green parts on the properties of a Graphite-5.5 vol. % Molybdenum- 0.6 vol. % Titanium composite obtained by Spark Plasma Sintering (SPS). The composite, sintered at 2000 ºC, below the eutectic temperature of the C-Mo system (2584 ºC), exhibits anisotropic properties depending on the direction of the applied pressure in the SPS machine. It has been proved that samples uniaxially pressed at 60 MPa to obtain the green compact exhibit highly improved properties compared with those obtained at lower pressure, which are competitive with those obtained under extreme conditions, i.e. uniaxial pressure at 300 MPa and sintering temperature > 2000 ºC in the presence of a liquid phase. The composite production process could be easier scaled up to the industrial level. Therefore, this graphite-molybdenum-titanium composite could be used as heat sink in a panoply of applications.

Keywords: Graphite; Spark Plasma Sintering; Thermal conductivity; Mechanical properties; Electrical conductivity

Corresponding authors:
[*] m.suarez@cinn.es (M. Suárez)
[†] d.fernandez@cinn.es (D. Fernández-González)

1. Introduction

Nowadays, there is a great need of design heat sinks more and more small, light, and efficient for their application in the most advanced emerging technologies, i. e. high performance electronic devices, mobiles, aerospace, high-speed trains, etc. In these regards, design parameters, raw materials as well as their thermal characteristics play an important role to obtain materials with great capacity to dissipate heat. From the typical materials as heat sinks, those based on the carbon stand out.

Graphite is a crystalline form of the element carbon where atoms are arranged in a hexagonal structure. This material exhibits good thermal and electrical conductivities, which are the reason of its application in electrodes, batteries, heat sinks, etc. However, it is also used in refractories, steelmaking, lubricants, and some other different applications.

The addition of reactive metals to strengthen carbons and graphite have been subject of research from at least 50 years. Mixtures of graphite-metal (particularly niobium, molybdenum, hafnium, tantalum, etc.) were studied to evaluate thermal-mechanical properties [1], [2], [3], [4], [5], [6], [7], [8], [9]. More recent research mainly focuses on the composites of copper or aluminum and graphite. Etter et al. [10] studied strength and fracture toughness of graphite-aluminum ($AlSi_7Ba$ and $AlSi_{12}$) composites produced by indirect squeeze casting process, enhancing flexural strength and fracture toughness. Etter et al. [11] also produced graphite/aluminum composites by gas pressure infiltration of aluminum alloys with varying silicon content into porous graphite preforms. Dewidar and Lim [12] studied copper-graphite composites produced by high frequency induction heating sintering using 2.5-15 wt. % graphite. Prieto et al. [13] manufactured and studied graphite flakes/metal composites aimed at being used in thermal management applications. They studied mixtures of graphite flakes with carbon fibers, Al-12Si and Ag-3Si with interesting values of thermal conductivity and coefficient of thermal expansion if compared with those of other carbon-based materials. Hutsch et al. [14] made metal matrix composites by powder metallurgy with carbon-based (natural graphite flakes) reinforcements to improve thermal conductivity. They prepared Cu-C, Al-C, Fe-C and W-C composites. Chen and Huang [15] studied the thermal properties of aluminum-graphite (10-90 vol. %) composites obtained via vacuum hot process. They appreciated significant improvements in thermal conductivity with almost full densification. Mazloum et al. [16] also studied copper graphite (0-50 vol. %) composites by powder metallurgy method. They observed a product with high thermal and electrical conductivities and low thermal expansion coefficient and lubricating properties. Mazloum et al. [17] also studied mechanical properties on copper-graphite composites. Oddone et al. [18] studied light metal alloys (aluminum and magnesium) with graphite to obtain a product with low thermal expansion, low density, and high thermal conductivity. They observed that

specific thermal conductivity was >4 times higher than that of copper. Karzov et al. [19] studied a composite based on expanded graphite and copper, and they checked that incorporating 3 wt. % Cu into expanded graphite allowed an increase of thermal conductivity of 20% while further increases implied a decrease of the thermal conductivity. Nazeer et al. [20] studied the thermal and mechanical properties of graphite-copper and graphene oxide-copper composites with good results, although, in this case, copper matrix was used. Byun et al. [21] prepared copper-graphite (up to 30 wt. %) composites by electrochemical deposition and spark plasma sintering. Kovacik and Emmer [22] also studied electric and thermal conductivities on copper-graphite composites with good results when 25 vol. % graphite. Liu et al. [23] studied the microstructure and properties of copper-graphite composites sintered using spark plasma sintering, although graphite content reached a maximum of 2.5 wt. %. Xiao et al. [24] studied copper-graphite metal matrix composites prepared by powder metallurgy from cuprous oxide and graphite as raw materials. Obtained composites exhibited better mechanical properties as well as better electrical conductivity.

Recent research on the carbon-molybdenum system includes that of Mariani [25], who studied molybdenum-copper-diamond, molybdenum carbide-graphite and molybdenum carbide-graphite-carbon fibers composites to be used in collimators. Bertarelli and Bizarro [26] studied the high temperature sintering of variable proportions of molybdenum powders and ceramic materials (graphite, carbon fibers, silicon, silicon carbide or tungsten) with potential applications in particle accelerators. Other works include that of Guardia-Valenzuela et al. [27], which aims of studying different graphite-molybdenum-titanium mixtures to be used in the Large Hadron Collider at CERN due to their extraordinary thermal and electrical properties. As can be seen from the above bibliographic review, little attention has been paid to obtain graphite-molybdenum composites and the research was focused mainly on extremely demanding and specific applications, i. e. collimators for colliders, reaching extremely high temperatures where a liquid phase is formed.

The objective of the present research is to study the best conditions to obtain graphite-molybdenum-titanium composites to be used in less demanding and definite applications as heat sinks for high-speed rail or electronic devices. Therefore, the main goal is to study the influence of the degree of compaction of green bodies on the final properties of graphite-molybdenum-titanium composites sintered by spark plasma sintering technique without involving the presence of liquid phase.

2. Experimental procedure.

2.1. Materials and experimental.

Graphite, molybdenum, and titanium powders were used as starting material to prepare the 93.9 vol. % graphite, 5.5 vol. % molybdenum and 0.6 vol. % titanium composite. This composition was chosen with the aim of comparing results with those obtained by Guardia-Valenzuela et al. [27].

Graphite (purity of 99%) from Asbury Carbons Company was used in the experiments. It consisted of crystalline natural graphite with spheroidal-flake morphology, with a mean particle size (d_{50}) of 30 μm (mode: 10-80 μm). The morphology of the graphite reduces the anisotropy of the final material and makes easier the compactness [25]. Particularly the spheroidal morphology allows a good mixing of raw powders resulting in a greater compaction of the final composite. This last question will explain some of the final properties of the material.

Molybdenum (purity of 99.5%) from H. C. Starck was used in the experiments. It consisted of spherical particles with a mean particle size (d_{50}) of 5.5 μm (mode: 3.5-5.5 μm).

Titanium (purity of 99.5%) from Abcr GMbh was used in the experiments. It consisted of titanium powder with irregular morphology, with a particle size < 45 μm.

The powder mixture was prepared in a high energy attrition mill (Union Process Inc. USA) using 3 mm alumina balls and a rate of 45 Hz. First, molybdenum and titanium powder were mixed in a roller mill with alumina balls for 24 hours with the aim of promoting the maximum contact between both metals. Then the mixture was charged into the high energy attrition mill with the graphite and it was mixed for 3 hours. Mixture was prepared using isopropyl alcohol to facilitate the mixing and ensure a homogeneous material for later operations. Finally, the material was dried at 100 °C and was sieved with a mesh of 125 μm.

Green compacts were obtained by uniaxial pressure in a metallic mould and then placed into a graphite die (40 mm inner diameter) to be sintered by Spark Plasma Sintering equipment to obtain samples with high density and good electrical and thermal conductivities. The cycle of the process consisted in heating at a rate of 25 °C/min from room temperature to 1400 °C and at 10 °C/min from 1400 °C to sintering temperature (2000 ºC), and finally, sample was sintered for 15 minutes of dwell time at 2000 °C. A uniaxial pressure of 30 MPa was applied during the sintering process. Temperature was controlled by an axial pyrometer focused on the upper graphite punch measuring the temperature above the sample center

2.2. Characterization techniques.

Microstructural characterization of Graphite-Molybdenum-Titanium powders and sintered samples was performed by Field Emission Scanning Electron Microscopy (FESEM) on a Quanta FEG 650.

Mineralogical phases were analyzed using X-ray diffraction technique using a Bruker Advanced Powder X-ray diffractometer model D8 with Cu-kα radiation (λ = 0.15406 nm). Working conditions included copper anticathode water cooled with an intensity of 40 mA and a voltage of 40 kV, a swept between 10-70° with a step of 0.02° and a step time of 0.2 s. To evaluate the molybdenum carbide formation, high temperature X-ray diffraction analysis was run in a thermodiffractometric (TDX) studies were carried out on a Bruker D8 Advance Vantec diffractometer equipped in vacuum with an HTK 2000 variable temperature chamber (Germany). Patterns were obtained using Cu Kα radiation. The measurements were made in the 10º-70º range and the step size and time of reading were 0.02º and 0.2 s, respectively, at measurement intervals of 50 °C. The temperature ranged from room temperature to 1200 °C, with a heating rate of 10 °C/min. In both X-ray diffraction analysis, the identification of the crystalline phases was realized by using diffraction pattern files provided by JCPDS (International Centre for Diffraction Data).

Relative density of the sintered samples was determined by geometric model using **equation (1).**

$$\rho\ (\%) = {}^{d}/_{d_r} \cdot 100 \qquad \text{Eq. (1)}$$

where d is the measured-apparent density and d_r is the real density obtained by helium pycnometer using AccuPyc 1330 V2.04N.

Mechanical properties were tested in mechanical tests machine Shimadzu-Serie AGS-IX. Samples of 3x4x20 mm were prepared to evaluate the flexural resistance. Bending strength of materials after the three-point bending test was evaluated using **equation (2)**:

$$\sigma_f = {}^{3 \cdot P \cdot L}/_{2 \cdot w \cdot b^2} \qquad \text{Eq. (2)}$$

where σ_f is the bending strength of the material in MPa, P is the failure load in N, L is the distance between supports (span) in mm, w is the width of the sample in mm and b is the thickness of the sample in mm.

Electrical conductivity was determined by four-point probe measurement, using the equipment PSM1735 - NumetriQ - Newtons 4th. In this sense samples of 3x4x20 mm were prepared to evaluate the electrical conductivity. Four equidistant conductive contacts (1.386 mm) were

located on the sample in-plane and out-of-plane. The resistivity was determined using the **equation (3)**:

$$\rho = \mathrm{F}\left({}^{w}/_{s}\right) \cdot {}^{\pi}/_{ln2} \cdot \mathrm{w} \cdot {}^{V}/_{I} \qquad \text{Eq. (3)}$$

where w is the thickness of the sample (cm), ρ is the bulk resistivity (Ω·cm), s is the pin spacing of four-point probe (cm), V/I is given by the equipment, and F(w/s) is calculated according to the **equation (4)** for thick substrates and $\mathrm{F}(\mathrm{w}/\mathrm{s}) = 1$ for thin substrates.

$$\mathrm{F}\left({}^{w}/_{s}\right) = {}^{1.386}/_{\left({}^{w}/_{s}\right)} \qquad \text{Eq. (4)}$$

Finally, the electric conductivity σ is obtained following the **equation (5)**:

$$\sigma = {}^{1}/_{\rho} \qquad \text{Eq. (5)}$$

Young's modulus of sintered samples was determined with the equipment Grindsonic (MK, Belgium). Samples of 3x4x20 mm were prepared to evaluate this property and the measurement was made in-line and out-of-line.

Thermal conductivity is an indirect measurement, and it is calculated from the thermal diffusivity and the specific heat using the **equation (6)**:

$$\lambda = \alpha \cdot \rho \cdot c_p \qquad \text{Eq. (6)}$$

where λ is the thermal conductivity (W/m·K), α is the thermal diffusivity (mm^2/s), ρ is the density (g/cm^3) and c_p is the specific heat (J/g·K). The measurement of the thermal diffusivity was carried out in the equipment LFA 457 MicroFlash from Netzsch at 25 ºC. For measuring, the samples were cut to obtain 10x10 mm square sections with a thickness of approximately 3 mm. Specific heat was determined to calculate the thermal conductivity using a C80 (Setaram Instrumentation) calorimeter equipped with stainless steel cells (S60/1413). Specific heat determination is carried out in continuous mode, using a heating ramp of 0.1 ºC/min from 20 to 40 ºC, with 2 hours of stabilization at the start and end temperatures. The data processing was carried out using the Calisto Software.

As the thickness of the sintered samples was insufficient to make direct measurements of the thermal conductivity in the plane/face perpendicular to the pressing direction (referred to in-plane), thermal conductivity was indirectly determined by means of the Wiedemann-Franz law. This law establishes that:

$$\lambda/_{\sigma} = L \cdot T \qquad \text{Eq. (7)}$$

where λ is the thermal conductivity, σ is the electrical conductivity, L is the Lorenz number and T is the temperature. It is assumed that the Lorenz number is the same it does not matter the direction without significant error.

3. Results

3.1. Density

To study the influence of the green density on the final properties of the SPS sintered samples, mixed powders were subjected to different pressure values. According to results showed in **Figure 1** three values of pressure were selected: 15, 40 y 60 MPa since a compaction at higher pressures did not involve a significant change in the value of the density of the green compacts. These values of pressure were significantly lower than those used in Guardia-Valenzuela et al. [27] (300 MPa).

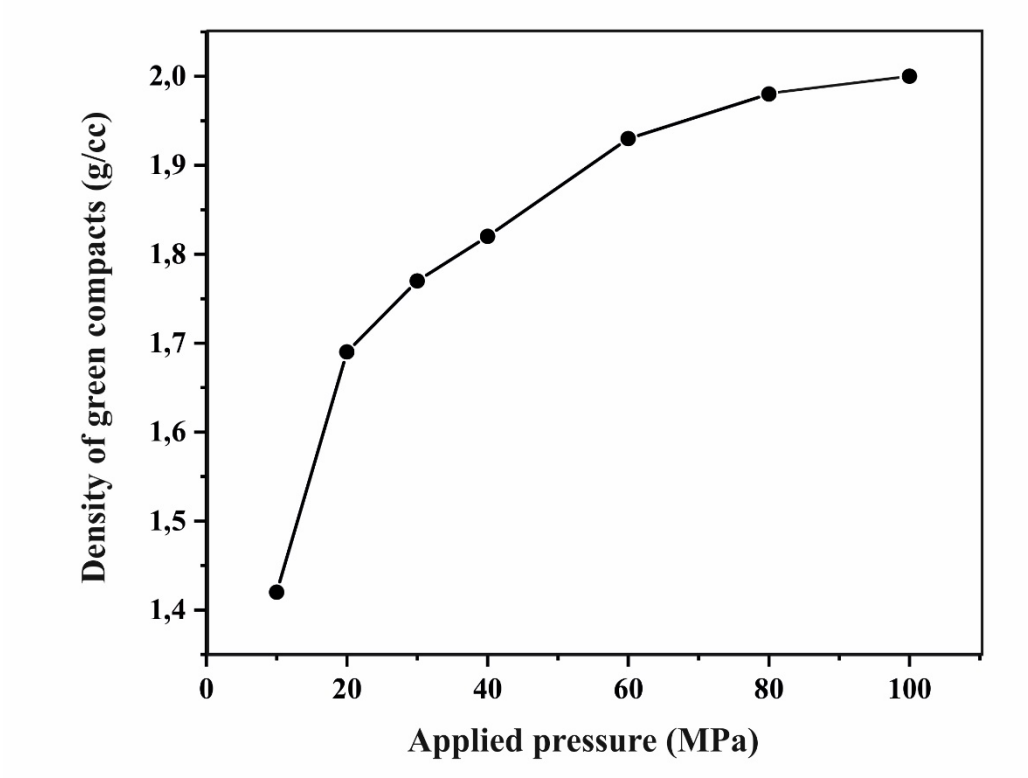

Figure 1. Variation of the green density vs the applied pressure.

Relative density of the sintered powders was calculated using **equation (1)** and the values are shown in **Table 1**. The pressure applied to obtain the green compacts before the sintering by SPS allows a greater green density (see **Figure 1** and **Table 1**) and, subsequently, a greater density after the sintering process. In the case of samples compacted at lower values of uniaxial pressure, they exhibit low values of densification (<90%) that involve the presence of voids/pores, which significantly reduce the properties of the sintered product. Within this context, densification improves significantly when the applied pressure is increased to obtain the green compacts. This way, when the uniaxial pressure applied is 60 MPa, the relative density exceeds 95%, with few pores/voids, which justifies the better properties with respect to those of the samples subjected to uniaxial pressing at 15 and 40 MPa.

Table 1. Density values of the green compacts, apparent density and relative density.

Uniaxial pressure (MPa)	Green density (g/cm^3)	Apparent density sintered (g/cm^3)	Relative density sintered (%)
15	1.46	2.29	81.1
40	1.82	2.43	87.5
60	1.93	2.55	95.3

3.2. Electrical conductivity

In the case of the electrical conductivity, it is well known that graphite exhibits better properties in the basal plane than in the perpendicular direction. Thus, the electrical conductivity was measured in-plane and in the plane parallel to the pressing direction (referred to out-of-plane). Results are shown in **Table 2.**

Table 2. Electrical conductivity values of the SPS-samples.

Uniaxial Pressure (MPa)	Electrical conductivity (MS/m, in-plane)	Electrical conductivity (MS/m, out-of-plane)
15	0.11	0.08
40	0.13	0.09
60	0.86	0.22

As will be seen, graphite exhibits a typical axial behavior: properties are usually better in the basal plane than in the perpendicular plane although graphite with spherical flake morphology was used in these experiments. This way, using low pressures to obtain green compacts, there is not accommodation of the basal planes of the graphite grains until all of them are in the same direction. Nevertheless, this is not the case of the green compacts obtained at greater pressures (60 MPa), where graphite grains have the highest degree of preferential orientation of all samples. In this manner, properties are significantly better in the samples where greater values of uniaxial pressure were applied.

The anisotropic behavior makes that values of electrical conductivity are consistent with those provided by Guardia-Valenzuela et al. [27] for Thermal Pyrolytic Graphite (2.4 MS/m in-plane, 0.07 MS/m in the perpendicular direction) and other composites of the group Graphite-Molybdenum-Titanium (0.88-1.01 MS/m in-plane, 0.08-0.07 MS/m in the perpendicular direction). In the case of samples pressed at 60 MPa to obtain green compacts the values are: 0.86 MS/m in-plane, 0.22 MS/m out-of-plane. Although in-plane, electrical conductivity is almost three times greater than in the case of other composites of the group, this value indicates that graphite planes are not completely oriented in the direction perpendicular to the pressing. In the case of samples pressed at 15 and 40 MPa, values are extremely low if compared with those above-mentioned. It is necessary to take into account that the responsible of the electrical (as well as thermal) conductivity is the matrix constituent, in this case graphite. The low values of densification (**Table 1**) are consequence of the presence of pores/voids/holes on the composite's microstructure. Since electrical conductivity is significantly reduced in the presence of this defects, electrical conductivity values are very low in the case of the samples with low degree of compaction.

3.3. Young's modulus

Young's modulus values were determined in both directions and the results are collected in **Table 3**. The values of the Young's modulus depend more on the presence of defects (pores) than on the direction where they are measured and, for that reason, significant differences are not clearly appreciated in the case of the sample uniaxial pressed at 60 MPa.

Table 3. Values of the Young's modulus of the SPS-samples.

Uniaxial Pressure (MPa)	Young's modulus (GPa, in-plane)	Young's modulus (GPa, out-of-plane)
15	31.42 ± 0.0	71.11 ± 0.2
40	32.98 ± 0.2	78.20 ± 0.2
60	74.05 ± 0.2	78.54 ± 0.1

3.4. Thermal conductivity

Thermal conductivity was indirectly measured from thermal diffusivity and specific heat values, and its value is calculated from **Equation 3** in the perpendicular direction to the basal plane (out-of-plane). Results are collected in **Table 4**. However, the diffusivity cannot be determined in the direction perpendicular to the applied pressure using the Netzsch LFA 457 MicroFlash, due to the dimensions of the samples. Therefore, we use the Wiedemann-Franz law to determine the thermal conductivity through the electrical conductivity. The Lorenz Number is assumed to be the same it does not matter the direction (values are shown in **Table 5**). Therefore, values of the thermal conductivity in the basal plane are collected in **Table 5**.

Table 4. Values of the thermal conductivity in the perpendicular direction to the basal plane at 25 ºC.

Uniaxial Pressure (MPa)	Cp (J/g·K)	Thermal diffusivity (mm^2/s)	Thermal conductivity (W/m·K, out-of-plane)
15	0.68	10.08	15.66
40	0.63	9.80	15.12
60	0.59	15.56	23.43

Table 5. Values of the thermal conductivity in the basal plane at 25ºC.

Uniaxial Pressure (MPa)	Lorenz number ($W \cdot \Omega/K^2$)	Thermal conductivity (W/m·K, in-plane)
15	$9.788 \cdot 10^{-6}$	21.53
40	$8.400 \cdot 10^{-6}$	21.84
60	$5.325 \cdot 10^{-6}$	91.59

Guardia-Valenzuela et al. [27] report that the thermal conductivity of Thermal Pyrolytic Graphite (TPG) in-plane is 1685 W/mK and in perpendicular direction is 8 W/mK at room temperature, while for graphite-molybdenum-titanium in-plane is 647-740 W/mK and in perpendicular direction is 56-50 W/mK at room temperature. In our case, the thermal conductivity values in the perpendicular direction are still better in the case of TPG, but in the case of the basal plane they worsen. Thermal conductivity depends on the presence of pores/voids/holes (low values of densification) and also the degree of alignment of the graphite and the bonds between graphite grains. In this sense, the value of this property is reduced in the case of porous materials and in the graphite composites compacted at lower pressures.

3.5. Bending strength

Bending strength was determined by means of the three points bending test. It is possible to check that there are not significant differences in resistance when considering the perpendicular or parallel to the pressing direction (**Table 6**). The best results achieved are, as in the other cases, using a uniaxial pressure of 60 MPa.

Table 6. Values of the Bending strength.

Uniaxial Pressure (MPa)	Bending strength (MPa, in-plane)	Bending strength (MPa, out-of-plane)
15	33.35 ± 0.6	32.23 ± 5.4
40	30.14 ± 8.9	34.48 ± 2.4
60	89.99 ± 3.1	101.68 ± 11.5

Mechanical strength is supported by the carbide-graphite bond, which is strong according to Guardia-Valenzuela et al. [27], providing bridges not only in the in-plane direction but also in the perpendicular direction and limits the basal plane slip (shear) and the delamination.

3.6. Microstructural characterization

The microstructure of the sintered samples subjected to different uniaxial pressure values was analyzed using the field-emission scanning electron microscope. It is possible to see in **Figure 2a-c** the micrographs of samples pressed at 15, 40 and 60 MPa, respectively. These images correspond to a cross-section of the sintered discs; this is the XXX direction. In the case of the

samples uniaxially pressed at 15 and 40 MPa, it is possible to appreciate that molybdenum (and titanium, bright color) carbide particles are not adequately distributed in the matrix of graphite (**Figures 2 a** and **b**), and the sizes close to 15-20 μm. Additionally, pores/voids/holes are identified although they are not clearly appreciated in the micrographs (densification was <90% in this two samples). In the case of the sample uniaxial pressed at 60 MPa, molybdenum (and titanium) carbide particles are more disaggregated and fairly distributed in the matrix of graphite (**Figure 2c**), with a particle size of 2-3 μm. This inadequate distribution of the molybdenum (and titanium) carbide particles in the graphite matrix, as well as the size and the greater degree of compaction, has a significant influence in the physical and mechanical properties of the graphite-molybdenum-titanium composite. As mentioned, carbides tend to elongate in the direction perpendicular to the pressing direction, but only in the case of the samples pressed to obtain green compacts at 15 and 40 MPa, and they have a greater size if compared with the situation at 60 MPa. This situation is not observed in the sample pressed at 60 MPa, where the microstructure is homogeneous. Repeatability of the microstructure was confirmed by taking micrographs in other sections of the sintered specimens.

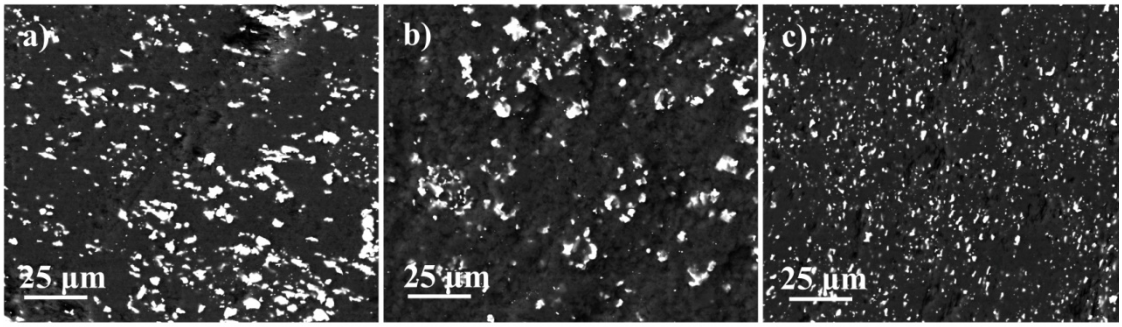

Figure 2. FESEM micrographs of the SPS-sintered graphite-molybdenum-titanium composites uniaxial pressed at 15 MPa (a), 40 MPa (b) and 60 MPa (c).

4. Discussion

Metal-graphite composites have been attracting interest for different applications particularly related to the thermal and electrical conductivities. Even if copper and aluminum composites can be used in this type of applications, from the mechanical point of view, these composites have limited interest when using them at high temperatures. Therefore, molybdenum-graphite composites are interesting because of their refractory character, the high thermal stability, the physical and mechanical properties as well as the thermal and electrical conductivities. On this latter point, Mo_2C (apart from exhibiting a great hardness [28], [29], [30], [31], [32]) has a metal-like electrical conductivity that confers capacity to conduct electricity to the composite. A high

temperature X-ray diffraction analysis was conducted to the sample before SPS sintered sintering to check the temperature at which Mo_2C phase starts to appear since it could confer the exceptional properties to the composite (**Figure 3**). Above 700 °C, the peak of the molybdenum (40.6°, 58.7°) is decreasing in intensity due to the formation of the molybdenum carbide (Mo_2C) (34.3°, 38°, 39.4°, 52°, 61.4°).

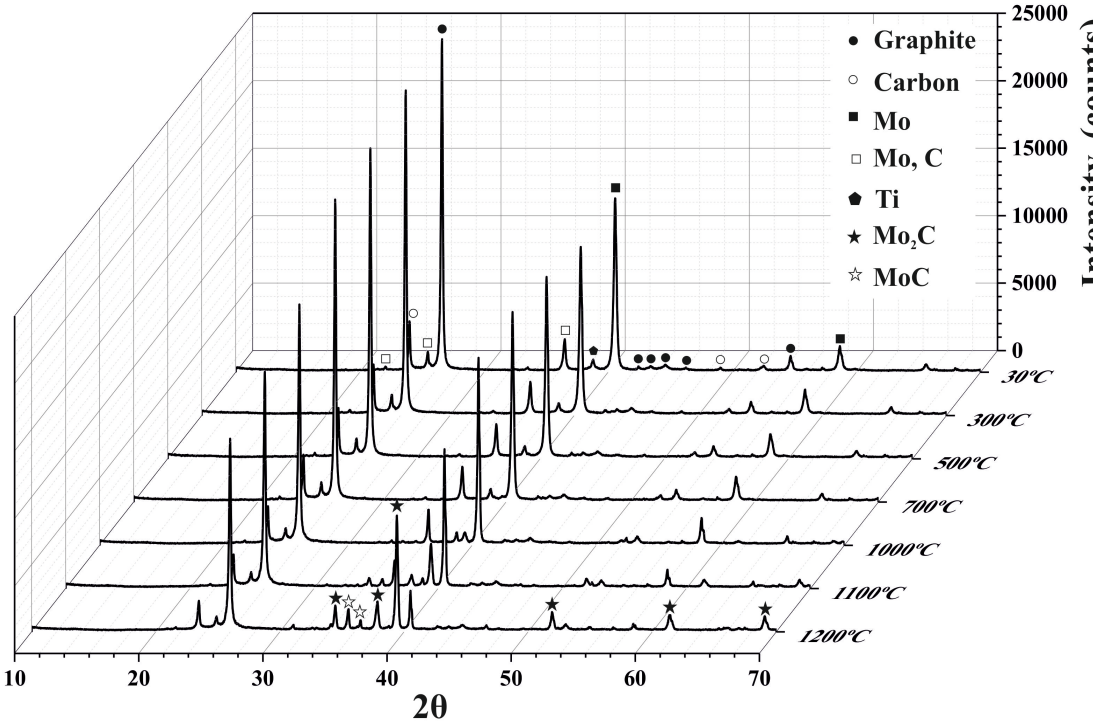

Figure 3. High temperature X-ray diffraction analysis of graphite-Molybdenum-Titanium.

However, after sintering in the SPS equipment, significant differences were observed with respect to the X-ray diffraction analysis presented in **Figure 3**. These differences explain some of the properties of the samples obtained in the present work. X-ray diffraction patterns are collected in **Figure 4,** where graphite and MoC are the main mineralogical phases.

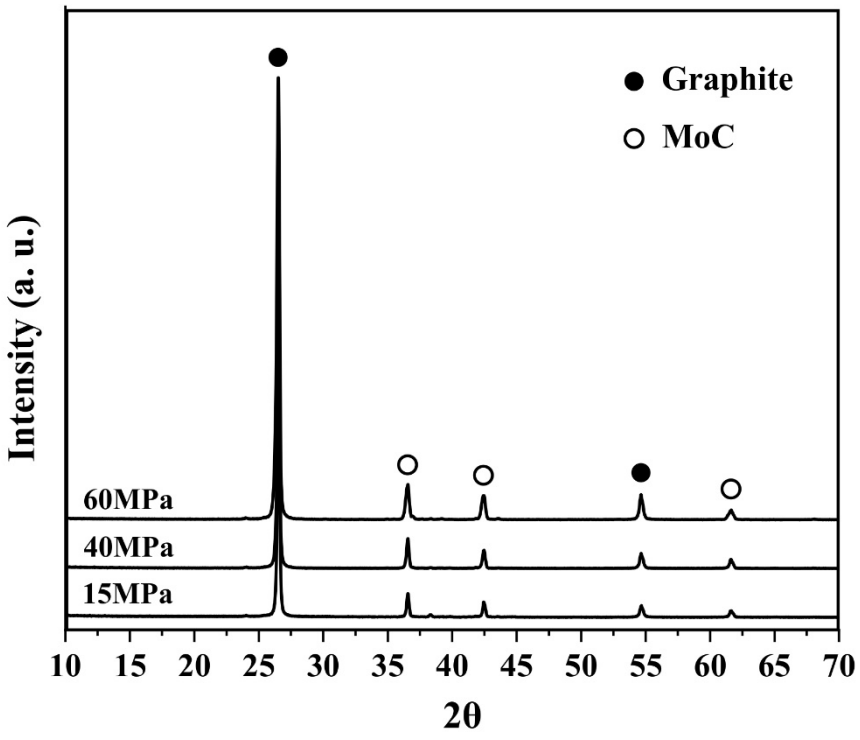

Figure 4. X-ray diffraction pattern of samples previously uniaxial pressed at 15, 40 and 60 MPa and then SPS sintered at 2000 ºC-15 min.

Molybdenum and graphite exhibit chemical affinity [25]. Therefore, when heating above 1000 ºC, hexagonal Mo_2C appears. This hexagonal structure is produced by the atomic diffusion of carbon atoms inside the molybdenum bcc lattice interstitials to form the hexagonal Mo_2C when the amount of carbon reaches 33 at. %. An important issue in the formation of the carbides is the diffusion processes. According to Matthews and Jenkins [33], carbon, being a relatively small atom, should travel rapidly through metal and carbide lattices via interstitial vacancies. On the other hand, the transport of metal atoms through graphitic materials is thought to be a comparatively slow and difficult process. Reaction of carbides formation continues by the diffusion of carbon inside Mo_2C and the formation of MoC. This explains the appearance of MoC in the samples. MoC can have positive influence in mechanical properties if it is adequately and finely distributed in the Mo_2C, as otherwise MoC at grain boundaries or in acicular form significantly reduces the final strength of the composite [25].

If we consider the Mo-C binary diagram, it is possible to see that sintering temperature (2000 °C) was not sufficient to reach the eutectic point as in the case of Guardia-Valenzuela et al. [27] (≃2600 °C, eutectic temperature 2584 °C). This means that sintering did not involve liquid phase

in our experiments, even considering that temperature in the central zone of the sample could be greater as temperature was measured by an optical pyrometer located outside of the sample. Anyway, temperature exceeded 1960 °C, because α-MoC_{1-x}, which is cubic, was formed in the three samples. Titanium titanium melts at 1670 ºC before reaching the sintering temperature of 2000 ºC, giving rise to a small fraction of transitory liquid that will immediately react with the carbon to form titanium carbide (TiC). Undoubtedly, this small fraction of the liquid phase can facilitate the transport of mass and therefore the sinterization of the composite during its brief appearance (as has been verified in works published in the literature [34]. Furthermore, the addition of titanium stabilizes α-MoC_{1-x} carbide (cubic, which is not stable below 1960 °C) and this justifies the presence of this carbide at room temperature. This is the main effect of titanium on the samples since it does not modify the eutectic temperature since the percentage of this element is very low. Another effect of titanium addition was the increase of graphitization. This matter is known since the sixties of the last century, as it was studied by several researchers that the additions of metals have been seen to catalyze graphitization of carbons [35], [36], [37].

It is possible to see in FESEM micrographs of **Figure 2** that because of the temperature, graphite particles-grains orient themselves perpendicular to the pressing direction, to exhibit the best properties in this direction. In these experiments, the objective is to study the effect of the initially applied pressure on the final properties of graphite-molybdenum-titanium composites. Thus, samples were uniaxial pressed before being treated in the SPS machine. Three pressures were considered (15, 40 and 60 MPa) to analyze this effect since studies of the densification at greater pressures did not significantly increase the densification of the sample (>95% relative density was achieved in the sample pressed at 60 MPa). The value of pressure has an effect on the distribution and grain size of the second phase and a possible explanation to this result could be that the pressure applied to the samples before sintering has an influence on the compaction of the green body as it is shown in **Table 1**, favours the breakdown of agglomerates, increasing the contact between the particles and favouring the sintering mechanisms. During sintering, different mechanisms can occur. Some of them favour densification and others the grain growth. If we considered the grains as inclusions and these inclusions increase the energy necessary for the movement of a grain boundary and inhibit grain growth, the higher number of grains the higher number of inclusions and the lower grain size in the sintered material.

Graphite is an anisotropic material and it is possible to see that properties are better the greater the pressure applied to obtain green compacts since in principle align more the graphite grains, and only when the pressure was >60 MPa, properties are, although lower, comparable with those of Guardia-Valenzuela et al. [27], where also liquid phase sintering was involved. Pressures <60 MPa to obtain green compacts are not adequate to obtain composites with good properties.

Moreover, there were no significant differences in the properties in the parallel or perpendicular directions to the pressing for samples obtained with these values of pressure. This could be related to the incomplete orientation of the graphite grains-particles until having most of the preferential planes in the direction perpendicular to the pressing. Also, there is not a complete densification when pressing at 15 and 40 MPa, which implied an important volume of pores/voids/holes, that are deleterious for all properties. It was demonstrated by Matthews [7] and Matthews et al. [38] that molybdenum as fine dispersed phase promoted by the hot deformation can effectively bond together graphite flakes in a composite to inhibit basal planes slip and the fracture of the composite at room temperature. Increasing the pressure, increased the preferred orientation of graphite basal planes and dispersed carbide phase strengthened natural graphite by bonding graphite flakes together to inhibit basal slip and fracture [7]. This represented a significant advance since bending strength can be substantially increased even in composites with graphite matrix, as it is the case of the composite of this research.

As opposed to Guardia-Valenzuela et al. [27], where a uniaxial pressure of 300 MPa was used to obtain the green bodies to be sintered in the SPS machine, in our experiments a maximum pressure of 60 MPa was used to obtain the green compact to be sintered. Additionally, on the contrary to the research of Guardia-Valenzuela et al. [27], the sintering temperature in these experiments was below the eutectic temperature of molybdenum with carbon (2584 °C) at temperature of 2000 °C. Therefore, sintering was carried without the presence of liquid phase. The forming conditions have an influence on the final properties of the sintered sample and, even if properties are lower than those obtained by Guardia-Valenzuela et al. [27], they are sufficient for the proposed application of heat dissipation, with easier upscaling (composites could be obtained at lower temperatures and pressures).

The main properties of this type of materials include high thermal conductivity, low density, excellent machinability conferred by the graphite matrix being suitable for complex geometrics machining. This could lead to the application of these materials in different fields including, diode lasers, power transistor substrate, LED substrate, wireless communication, electrical drivers, aerospace power supplies, medical electronic systems, avionics systems apart from heat sinks.

5. Conclusions

Graphite-molybdenum-titanium composites were sintered by Spark Plasma Sintering technique using different pressures to obtain green compacts and, in this way, studying the effect of the degree of compaction on the properties of the composite. Sintering, as opposed to other investigations, takes place in the solid phase, which is a challenge since the fabrication temperatures are much lower. This may represent a significant advance regarding the processing

requirements. Samples uniaxial pressed at 60 MPa exhibit highly improved results related to thermal, electrical, and mechanical properties compared with those obtained at lower pressure and also reasonably compete with those obtained under extreme conditions, i.e. uniaxial pressed at 300 MPa and sintering temperature > 2000 ºC in the presence of a liquid phase. In additions as a consequence, the composite production process could be easier scaled up to the industrial level. Therefore, graphite-5.5 vol. % Molybdenum- 0.6 vol. % Titanium composite could be used as heat sink in a panoply of applications.

Acknowledgements

This research was funded by the Spanish Ministry of Science and Innovation. Call Programa Estatal de I+D+i Orientada a los Retos de la Sociedad [RTI2018-102269-B-I00].

This research was also supported by a Juan de la Cierva Formación grant from the Spanish Ministry of Science and Innovation (MCINN) to Daniel Fernández-González [FJC2019-041139-I]. A. Borrell acknowledges for her RYC-2016-20915.

Authors are grateful to Ainhoa Macías San Miguel from Nanomaterials and Nanotechnology Research Center (CINN) for providing technical assistance.

References

[1] M. Humenik, D. W. Hall, R. V. Alsten, Graphite-base cermets: a new material for bearing, electrical and high-temperature applications, Met. Progr. 81 (1962) 101–108.

[2] J. White, R. Price, Hot-working of graphite for graphite-matrix nuclear fuels, Carbon 2 (1965) 327-330. https://doi.org/10.1016/0008-6223(65)90001-1

[3] J. White, J. Pontelandolfo, Graphite-carbide materials prepared by hot-working with the carbide phase in the liquid state, Nature 209 (1966) 1018-1019. https://doi.org/10.1038/2091018a0

[4] J. White, J. Pontelandolfo, Graphite-carbide materials prepared by hot-working with a dispersed liquid-carbide phase, Carbon 4 (1966) 305-314. https://doi.org/10.1016/0008-6223(66)90043-1

[5] J. White, J. Pontelandolfo, HWLC graphites prepared by hot-working extruded stock, Carbon 6 (1968) 1-2. https://doi.org/10.1016/0008-6223(68)90043-2

[6] Y. Harada, G. A. Rubin (1966): Fabrication and characterization of metal carbide-graphite composites, Presented at the 68th Annual Meeting of The American Ceramic Society, May 9, 1966, Washington, D. C.

[7] R. Matthews (1970): Deformation and Strengthening in Molybdenum Carbide - Natural Graphite Composite Materials, Ph.D. thesis, University of Wales.

[8] R. Staffler, G. Kneringer, E. Kny, N. Reheis, Metal/graphite-composites in fusion engineering, IEEE Thirteenth Symposium on Fusion Engineering, Knoxville, TN, USA, 1989, pp. 955-958, vol. 2, doi: https://doi.org/10.1109/FUSION.1989.102375

[9] D. John, G. M. Jenkins, Hot-working and strengthening in metal carbide-graphite composites, J. Mater. Sci. 21 (1986) 2941-2958. https://doi.org/10.1007/BF00551515

[10] T. Etter, J. Kuebler, T. Frey, P. Schulz, J. F. Löffler, P. J. Uggowitzer, Strength and fracture toughness of interpenetrating graphite/aluminium composites produced by the indirect squeeze casting process, Mat. Sci. Eng. A-Struct. 386 (2004) 61-67. https://doi.org/10.1016/j.msea.2004.06.066

[11] T. Etter, P. Schulz, M. Weber, J. Metz, M. Wimmler, J. F. Löffler, P. J. Uggowitzer, Aluminium carbide formation in interpenetrating graphite/aluminium composites, Mat. Sci. Eng. A-Struct. 448 (2007) 1-6. https://doi.org/10.1016/j.msea.2006.11.088

[12] M. M. Dewidar, J.-K. Lim, Manufacturing Processes and Properties of Copper—Graphite Composites Produced by High Frequency Induction Heating Sintering, J. Compos. Mater. 41 (2007) 2183-2194. https://doi.org/10.1177/0021998307074145

[13] R. Prieto, J. M. Molina, J. Narciso, E. Louis, Fabrication and properties of graphite flakes/metal composites for thermal management applications, Scripta Mater. 59 (2008) 11-14. https://doi.org/10.1016/j.scriptamat.2008.02.026

[14] T. Hutsch, T. Schubert, J. Schmidt, T. Weissgärber, B. Kieback (2010): Innovative Metal-Graphite Composites a s Thermally Conducting Materials, PM2010 World Congress – PM Functional Materials – Heat Sinks.

[15] J. K. Chen, I. S. Huang, Thermal properties of aluminum–graphite composites by powder metallurgy, Compo. Part B-Eng. 44 (2013) 698-703. https://doi.org/10.1016/j.compositesb.2012.01.083

[16] A. Mazloum, J. Kovacik, S. Emmer, I. Sevostianov, Copper–graphite composites: thermal expansion, thermal and electrical conductivities, and cross-property connections, J. Mater. Sci. 51 (2016) 7977-7990. https://doi.org/10.1007/s10853-016-0067-5

[17] A. Mazloum, J. Kovacik, A. Zagrai, I. Sevostianov, 2020. Copper-graphite composite: Shear modulus, electrical resistivity, and cross-property connections. Int. J. Eng. Sci. 149, 103232. https://doi.org/10.1016/j.ijengsci.2020.103232

[18] V. Oddone, B. Boerner, S. Reich, Composites of aluminum alloy and magnesium alloy with graphite showing low thermal expansion and high specific thermal conductivity, Sci. Technol. Adv. Mater. 18 (2017) 180-186. https://doi.org/10.1080/14686996.2017.1286222

[19] I. M. Karzov, O. N. Shornikova, S. V. Filimonov, A. P. Malakho, V. V. Avdeev, Cu-Expanded Graphite Composite Material Preparation and Thermal Properties, Eurasian Chemico-Technological Journal 19 (2017) 273-277. https://doi.org/10.18321/ectj671

[20] F. Nazeer, Z. Ma, L. Gao, F. Wang, M. A. Khan, A. Malik, Thermal and mechanical properties of copper-graphite and copper-reduced graphene oxide composites, Compo. Part B-Eng. 163 (2019) 77-85. https://doi.org/10.1016/j.compositesb.2018.11.004

[21] M. Byun, D. Kim, K. Sung, J. Jung, Y.-S. Song, S. Park, I. Son, 2019. Characterization of Copper–Graphite Composites Fabricated via Electrochemical Deposition and Spark Plasma Sintering. Appl. Sci-Basel. 9, 2853. https://doi.org/10.3390/app9142853

[22] J. Kovacik, S. Emmer, 2019. Cross property connection between the electric and the thermal conductivities of copper graphite composites. Int. J. Eng. Sci. 144, 103130. https://doi.org/10.1016/j.ijengsci.2019.103130

[23] J. Liu, K. Sun, L. Zeng, J. Wang, X.-P. Xiao, J. Liu, C. J. Guo, Y. Ding, 2020. Microstructure and Properties of Copper–Graphite Composites Fabricated by Spark Plasma Sintering Based on Two-Step Mixing. Metals-Basel. 10, 1506. https://doi.org/10.3390/met10111506

[24] Z. Xiao, R. Chen, X. Zhu, Z. Li, G. Xu, Y. Jia, Y. Zhang, Microstructure, and Physical and Mechanical Properties of Copper–Graphite Composites Obtained by In Situ Reaction Method, J. Mater. Eng. Perform. 29 (2020) 1696–1705. https://doi.org/10.1007/s11665-020-04646-8

[25] N. Mariani (2014): Development of Novel, Advanced Molybdenum-based Composites for High Energy Physics Applications, Ph. D. Thesis, Milan Polytechnic, Milan, Italy (Supervisor: Alessandro Bertarelli).

[26] A. Bertarelli, S. Bizzaro, (2016): Inventors; CERN - European Organization For Nuclear Research, Brevetti Bizz S.R.L., assignees. A Molybdenum Carbide / Carbon Composite And Manufacturing Method, Int. Pat. Appl. (2013), PCT/EP2013/072818.

[27] J. Guardia-Valenzuela, A. Bertarelli, F. Carra, N. Mariani, S. Bizzaro, R. Arenal, Development and properties of high thermal conductivity molybdenum carbide - graphite composites, Carbon 135 (2018) 72-84. https://doi.org/10.1016/j.carbon.2018.04.010

[28] D. Fernández-González, I. Ruiz-Bustinza, C. González-Gasca, J. Piñuela-Noval, J. Mochón-Castaños, J. Sancho-Gorostiaga, L. F. Verdeja, Concentrated solar energy applications in materials science and metallurgy, Sol. Energy 170 (2018) 520-540. https://doi.org/10.1016/j.solener.2018.05.065

[29] N. Shohoji, J. Badie, B. Granier, F. A. Costa-Oliveira, J. Cruz-Fernandes, L. Guerra-Rosa, Formation of hexagonal η-MoC_{1-x} phase at a temperature lower than 1660 °C by solar radiation heating under presence of excess free carbon, Int. J. Refractory Metals Hard Mater. 25 (2007) 220-225. https://doi.org/10.1016/j.ijrmhm.2006.05.004

[30] B. Granier, J. Badie, F. A. Costa-Oliveira, T. Magalhaes, N. Shohoji, L. Guerra-Rosa, J. Cruz-Fernandes, Carbide synthesis from graphite/molybdenum powder mixtures at sub-stoichiometric ratios under solar radiation heating to 1900 °C, Mater. Trans. 49 (2008) 2673-2678. https://doi.org/10.2320/matertrans.MRA2008202

[31] B. Granier, N. Shohoji, F. A. Costa-Oliveira, T. Magalhaes, J. Cruz-Fernandes, L. Guerra-Rosa, Carbide phases synthesised from C/Mo powder compacts at specified sub-stoichiometric ratios by solar radiation heating to temperatures between 1600 °C and 2500 °C, Mater. Trans. 50 (2009) 2813-2819. https://doi.org/10.2320/matertrans.M2009167

[32] E. Parthe, V. Sadagopan, The structure of dimolybdenum carbide by neutron diffraction technique, Acta Cryst. 16 (1963) 202-205. https://doi.org/10.1107/S0365110X63000487

[33] R. B. Matthews, G. M. Jenkins, The high temperature interaction between molybdenum and graphite, J. Mater. Sci. 10 (1975) 1976-1990. https://doi.org/10.1007/BF00754489

[34] P. Pena, P. Miranzo, J. S. Moya, S. De Aza. Multicomponent toughened ceramic materials obtained by reaction sintering Part 1 ZrO_2-Al_2O_3-SiO_2-CaO system. J. Mater. Sci. 20 (1985) 2011–2022. https://doi.org/10.1007/BF01112284

[35] C. Yokokawa, K. Hosokawa, Y. Takegami, Low temperature catalytic graphitization of hard carbon, Carbon 4 (1966) 459-465. https://doi.org/10.1016/0008-6223(66)90060-1

[36] J. C. Bokros, A. S. Schwartz, A model to describe neutron-induced dimensional changes in pyrolytic carbon, Carbon 5 (1967) 481-492. https://doi.org/10.1016/0008-6223(67)90025-5

[37] S. M. Irving, P. L. Walker, Interaction of evaporated carbon with heated metal substrates, Carbon 5 (1967) 401-402. https://doi.org/10.1016/0008-6223(67)90056-5

[38] R. B. Matthews, D. B.; Fischbach, G. M. Jenkins, Compaction and Hot Working of Natural Graphite-Molybdenum Carbide Composite, Proceedings of the Third S.C.I. Carbon Conference, London, 1970, 515-519.